Modeling decadal bed material sediment flux based on stochastic hydrology

Michael Bliss Singer and Thomas Dunne

Donald Bren School of Environmental Science and Management, University of California, Santa Barbara, California, USA

Received 3 October 2003; revised 28 December 2003; accepted 9 January 2004; published 18 March 2004.

[1] Estimates of decadal bed material sediment flux and net storage are derived by driving sediment transport calculations with a stochastic hydrology model. The resulting estimates represent the whole distribution of sediment flux based on natural variability in channel characteristics (gradient, width, and bed grain size) and the magnitude, duration, and interarrival time of flood events. A procedure for calibrating a fractional sediment transport equation of a commonly used form to bed material grain size distributions (BMGSDs) at cross sections is presented. The procedure was applied to the Sacramento River channel network to compute estimates of annual total and annual peak bed material discharges into and through the main stem over a 30-year period. Main stem bed material budgets were evaluated to identify reaches in states of net accumulation or scour. Simulations highlight large imbalances in sand and gravel storage throughout the Sacramento River, which can be explained by a combination of local hydraulics and BMGSDs and for which there is at least some empirical support. *INDEX TERMS:* 1815 Hydrology: Erosion and sedimentation; 1869 Hydrology: Stochastic processes; 1821 Hydrology: Floods; *KEYWORDS:* bed material transport, sediment budgets, stochastic simulation, Sacramento River

Citation: Singer, M. B., and T. Dunne (2004), Modeling decadal bed material sediment flux based on stochastic hydrology, *Water Resour. Res.*, *40*, W03302, doi:10.1029/2003WR002723.

1. Introduction

[2] Bed material flux is the transport of sediment that constitutes the riverbed. The variation in bed material flux along a river channel creates a spatial pattern of stored sediment. These storage patterns influence the formation of the channel (e.g., point bars) and its functioning (e.g., depth of flow over a portion of a cross section). Accordingly, sediment storage can be thought of as the prime determinant of channel morphology in alluvial channels and thus of flood conveyance and habitat conditions in a river reach.

[3] Long-term estimates of bed material sediment flux and storage in large rivers are required for various purposes ranging from applications in flood control (bed elevations) and river rehabilitation to research on sediment budgets and channel morphology. These estimates are generally reported as single values derived from sediment transport data with no assessment of the uncertainty in their calculation [e.g., *Milliman and Meade*, 1983; *Milliman and Syvitski*, 1992] or their inter-annual variation. *Dunne et al.* [1998] applied error propagation to sediment rating curve analyses of bed material and washload fluxes and reach accumulations in the Amazon basin. *McLean et al.* [1999] reported a 20-year record of bed load in a large gravel bed river with error analyses of measurements and rating curves. However, to our knowledge, there have been no attempts to represent inter-annual variability in load estimates specifically due to the hydraulics of a variable flow regime.

[4] Toward this end, we have calibrated a bed material transport formula with measurements from the Sacramento and other rivers, and connected it to HYDROCARLO, a stochastic model of streamflow in a channel network (M. B. Singer and T. Dunne, An empirical-stochastic, event-based model for simulating inflow from a tributary network: Theoretical framework and application to the Sacramento River basin, California, submitted to *Water Resources Research*, 2003) (hereinafter referred to as Singer and Dunne, submitted manuscript, 2003). We used the coupled models to estimate the frequency distributions, including the extrema and central tendency, of bed material discharge in various grain size classes over a period of decades. We applied this method at various cross sections along the main stem Sacramento River and at the mouths of its major tributaries, and thus developed a basinwide method for assessing the long-term influence of flood variability on bed material transport. To our knowledge, our decadal estimation of the spatial variability of sediment transport at large basin scale is unprecedented.

[5] Many studies have acknowledged the inaccuracies in sediment transport prediction arising from uncertainty in hydraulic variables [*McLean*, 1995], spatial distribution of bed shear stress [*Wilcock*, 1996], and assessment of critical shear stress [*Wilcock*, 1992; *Buffington and Montgomery*, 1997]. Additionally, variations in local bed material grain size distributions (BMGSDs) due to patch dynamics [e.g., *Paola and Seal*, 1995] or topographic variability across the stream control initial mobility of sediment, the quantity of each size available for transport, and thus transport rates. However, streamflow is an additional source of uncertainty introduced when one tries to obtain a decadal estimate of bed material flux. The sensitivity of bed material flux to streamflow is apparent in regressions of the logarithm of bed material flux on the logarithm of stream discharge, which

0043-1397/04/2003WR002723$09.00

generally result in exponents greater than one. Even if one could properly constrain each of the aforementioned variables for a given set of flow conditions, it would still be necessary to properly characterize the stochastic frequency, magnitude, and duration of flow at a given cross section, in order to obtain an appropriate estimate of long-term bed material flux. Such a strategy is particularly important to determine the role of floods and their management in sediment transport and channel formation, and for assessing riverine habitat condition. The influence of historical streamflow on sediment transport estimates has been assessed empirically by convolving bed load ratings with flow frequency curves [*McLean et al.*, 1999]. We build on this research by stochastically simulating a range of flows and assessing their influence on decadal bed material transport.

[6] Long-term sediment flux prediction that incorporates the real variability inherent in the hydrology of a fluvial system would be useful on the scale of a cross section where computations are made (e.g., to evaluate local adjustment to a rehabilitation strategy) and that of a basin as a whole (e.g., to assess a the influence of system-wide perturbations on the sediment budget). In order to design a gravel augmentation strategy on the local scale, for example, it would be useful to quantify the central tendency and extrema of spawning-sized gravel transport past a particular cross section. On the basin scale, it would be useful to assess the influence of land-use change (e.g., an increase in sand loading to the channel) on bed material transport in various grain sizes throughout the main stem. This paper outlines a basinwide method for quantifying the variations in bed material transport over a period of decades punctuated by flood events of variable frequency, magnitude, duration, drawdown rate, and interarrival time.

[7] We perform the following at main stem and tributary cross sections along the Sacramento River: (1) stochastically simulate many realizations of daily flow sequences for 30 years (Singer and Dunne, submitted manuscript, 2003); (2) simplify cross-sectional geometry and calculate hydraulic variables for the cross section; (3) obtain the BMGSD from bulk material surveys; (4) determine dimensionless critical shear stress from local bed load measurements (where available); (5) derive a fractional bed material sediment transport equation of common form that incorporates local critical shear stress and prediction in distinct portions of a cross section; (6) calibrate the transport equation to various bed load data sets; (7) calibrate the equation to local BMGSDs; (8) simulate daily bed material flux for 30 years in various grain size classes; (9) combine long-term bed material flux estimates with prior estimates of long-term suspended sediment discharge [*Singer and Dunne*, 2001] at main stem locations to evaluate the contribution of bed material flux to total load; and (10) construct bed material sediment budgets for reaches of the Sacramento fluvial system. In this paper, we refer to sand and gravel transported from and along the riverbed as bed material load. We use the term bed load to refer to measurements made using a Helley-Smith sampler (see below).

2. Study Basin

[8] The Sacramento River has a basin of approximately 70,000 km^2, and the river flows from its headwaters near Mount Shasta through the northern Central Valley to the San Francisco Bay-Delta in California. It is controlled at the northern end by Shasta Dam, built in 1943. The Sacramento exhibits a range of fluvial environments. From Shasta Dam, it winds southward through Sacramento Canyon, incises into Pleistocene deposits on the Redding plain, and arcs through Iron Canyon to Bend Bridge (BB in Figure 1). This part of the river, labeled reach 0 (Figure 1), is ~40 km in length, has a bed of sandy gravel (~25% sand in bed material at BB), width of ~150 m, slope of ~8.9×10^{-4}, and point bar topography. From corroborated (K. Buer, CDWR, personal communication) field observations, we determined that 50% of the bed in reach 0 consists of the erosion-resistant Tehama formation. South of Bend Bridge the Sacramento enters the Central Valley, where it meanders across a wide floodplain through Pleistocene river gravels to Hamilton City (HC). Reach 1 is ~60 km in length, with a gravel and sand bed (~40% sand at HC), width of ~200 m, and slope of ~5.4×10^{-4}, with shallow cross sections and ~2 m natural levees. Downstream of Hamilton City, the Sacramento continues meandering through the valley, but is partially constrained by flood control levees, which influence the river's course beginning upstream of Butte City (BC). Reach 2 is ~30 km in length, consists of similar bed material (~49% sand at BC), cross-sectional topography, and width as reach 1, but with a lower slope (~2.5×10^{-4}). Below Butte City the Sacramento enters a reach where flood control levees are set back ~1 km from the channel until Colusa (CO). Reach 3 is ~25 km in length, consists of a sand bed (~75% sand at CO), width and cross sectional topography similar to the upstream reaches, and a slope of ~2.3×10^{-4}. It is controlled at the downstream end by an eastward deflection around the Colusa Dome, the result of a magmatic intrusion 1.4–2.4 Mya, which forces overbank sequestration of water and deposition of fine sediment [*Singer and Dunne*, 2001]. Downstream of Colusa the Sacramento is incised into the Pleistocene deposits of the Cache Creek fan and is completely constrained by flood control levees built on channel banks to Knights Landing (KL). This reach 4 is ~55 km in length, has no connected tributaries, a sand bed (~73% sand at KL) with lenses of gravel, width of ~100 m, largely symmetrical cross sections, and slope of ~1.0×10^{-4}. The Sacramento River below Knights Landing continues south to Sacramento (SA), where the river is influenced by tides. Reach 5 is ~30 km in length, consists of a sand bed (99% fine sand and silt at SA) and a gradient of ~0.8×10^{-4}.

[9] Herein we compute sediment discharge at cross sections that bound these river reaches and directly correspond with gauging stations for which we previously made long-term estimates of suspended sediment transport [*Singer and Dunne*, 2001]. Most cross sections used in this study have fixed widths over the range of moderate-to-high flows due to combinations of flood control levees, riprap, and revetment.

[10] The tributaries of the Sacramento flow from four geologic provinces, each of which is assumed to deliver a uniform sediment yield per unit drainage area. We compute bed material transport into the Sacramento from each tributary in a province by computing the load for a signature tributary in the province and scaling it by the ratio of drainage areas for the remaining tributaries. The signature

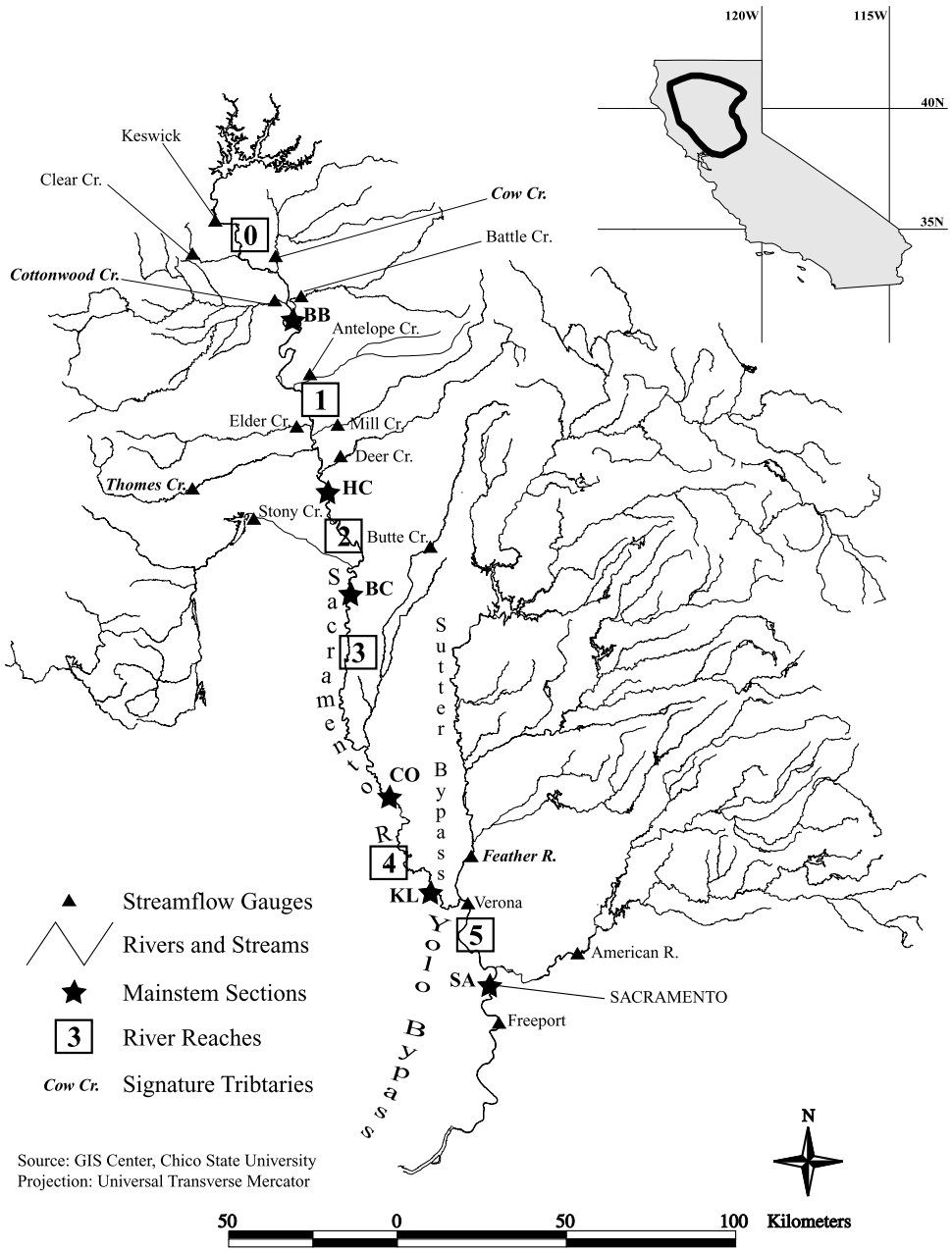

Figure 1. Map of study basin showing streamflow gauges used for stochastic flow simulation, stream network, main stem sections through which bed material transport was computed, river reaches for which simple sediment budgets were evaluated, and signature tributaries used to compute sediment entering the main stem from common geologic provinces (scaled by drainage area). Sutter and Yolo Bypasses are wide, off-channel floodways used to convey high flows.

tributaries for this study are Cottonwood Creek, Cow Creek, Thomes Creek, and Feather River, draining the Trinity Mountains, Modoc Plateau, Coast Ranges, and Sierra Nevada, respectively.

3. Data

[11] We employ channel cross sections extracted from high-resolution (~0.7 m contours) digital terrain models of the main stem Sacramento provided by the US Army Corps of Engineers (USACE) and the California Department of Water Resources (CDWR). These data sets were obtained by bathymetric surveys in 1997 and 2000, respectively. Together, they form a seamless set of contemporaneous (within 3 years) cross sections through which flow routing and sediment transport may be computed. Flow data from the Sacramento's major tributary gauges were obtained from the US Geological Survey (USGS) as described by Singer and Dunne (submitted manuscript, 2003). To define grain size distributions and to calibrate bed material transport formulae, we use bed load and suspended load data from USGS gauging stations, BMGSDs from USGS and CDWR bulk material surveys collected for main stem Sacramento River stations between 1977 and 1980, and one bed material

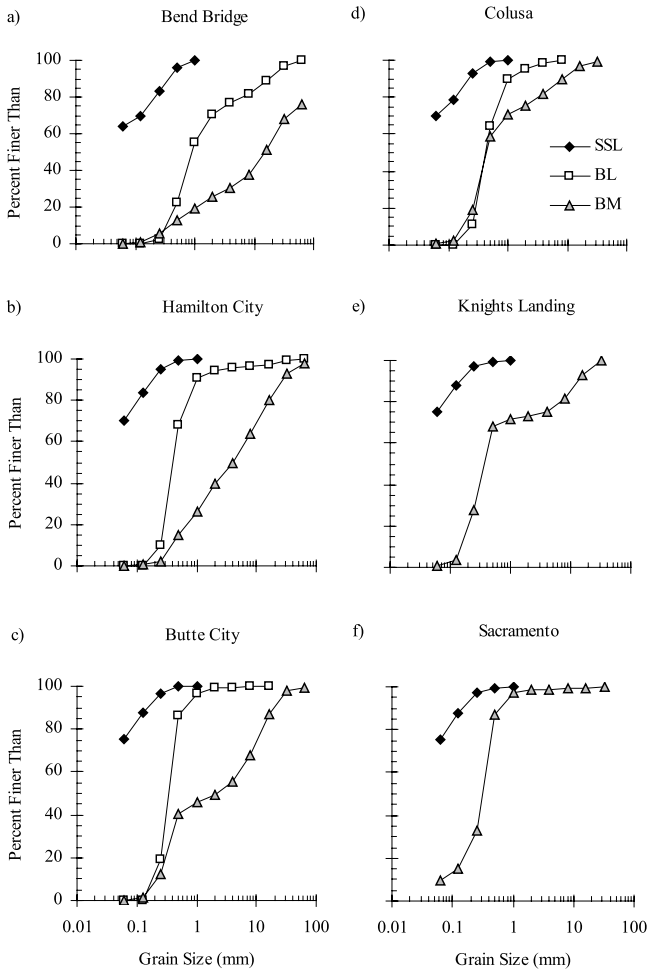

Figure 2. Grain size distributions of suspended load (SSL), bed load (BL), and bed material (BM) for the six main stem cross sections. Suspended load curves are generated from >10 samples. Bed load curves are generated from between 5 and 25 samples. Bed material curves are generated from between 1 and 20 samples.

sample that we collected in 2003 from a point bar at Bend Bridge. These data are presented in Figure 2.

4. Stochastic Hydrology Model

[12] In order to drive the sediment transport calculations, we developed a stochastic hydrology model that simulates inflow to the main stem of a large river from its major tributaries by semi-random sampling of tributary flood events. The model, HYDROCARLO (Singer and Dunne, submitted manuscript, 2003), produces roughly synchronous inflow from tributaries by replicating empirical patterns in flood occurrence and correlation in flood peak magnitude between most tributary gauges. In applying it to the Sacramento River basin, we demonstrated the overwhelming influence of basinwide storms that induce synchronous flood conditions at all tributary gauges. We also showed that the model produces plausible patterns of tributary inflow which, when routed through the main stem produce hydrographs with median characteristics (e.g., peak, duration, interarrival time) similar to those of observed main stem hydrographs. However, the model also provides extrema of frequency distributions, which can be useful for computing sediment transport for a range of conditions that may not be represented in main stem hydrologic records and for forward modeling under changed hydrologic conditions.

[13] In this sediment transport study, we used HYDROCARLO to simulate daily inflow to the main stem Sacramento River for a 30-year period that represents the hydrology of the era since the construction of Shasta Dam. We routed this inflow through the main stem to each of the selected cross sections (Figure 1) using the flow routing software, HEC-RAS, and extracted mean daily flow stage for the duration of each 30-year simulation. We conducted 50 such simulations to stochastically represent a large range of flood events in the basin and to converge on extrema and central tendency of bed material flux associated with them.

5. Cross-Sectional Geometry and Hydraulics

[14] Bed material flux may differ in distinct portions of a river channel cross section. In our one-dimensional calculations we try to capture those differences in flow depth that lead to spatial variability in shear stress [*Wilcock*, 1996]. For example, bed shear stresses are higher in the thalweg than on a high bar surface, for the same BMGSD. Therefore calculating rates of sediment transport for an entire cross section based on mean flow depth introduces inaccuracies into the results. We have simplified the geometry for each of our cross sections to represent the varying depths that could lead to differential transport rates in distinct portions of the section based on a single cross-sectional flow stage. We divided cross sections into portions, each with its own elevation datum and width (Figure 3). We acknowledge that there may be cross-stream variations in BMGSD [e.g., *Paola and Seal*, 1995] that are not being represented for lack of data.

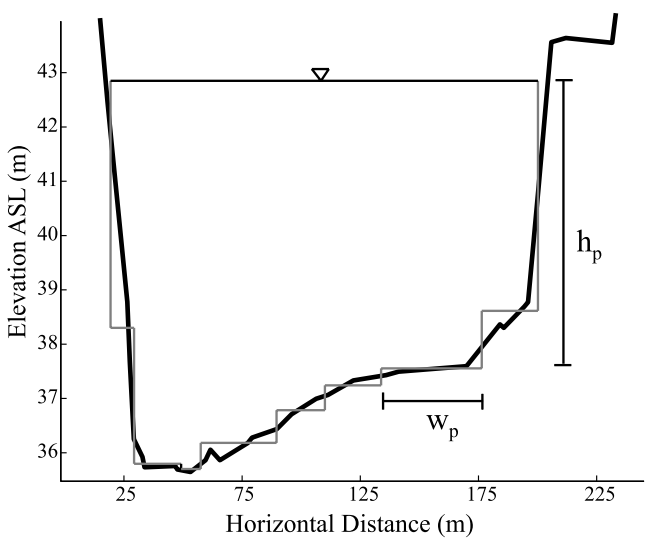

Figure 3. Plot of the cross section at Hamilton City illustrating the simplification of cross sections into seven distinct portions for which we computed hydraulics and sediment transport. Each portion, p, has a flow depth, h, and a width, w.

[15] We used daily flow elevation extracted from HEC-RAS to compute daily water surface slope, s, for the cross section as

$$s_x = \frac{\left(\frac{z_{x+1} - z_x}{c1} + \frac{z_x - z_{x-1}}{c2}\right)}{2} \quad (1)$$

where z is water surface elevation, the subscripts x, $x + 1$, and $x - 1$ denote the cross section average of the section in question, the next upstream section, and the next downstream section, respectively, $c1$ is the centerline distance between sections $x + 1$ and x, and $c2$ is the centerline distance between sections x and $x - 1$. Centerline distances between our selected cross sections on the Sacramento are ~800 m. Hereafter we refer to section-average quantities with the subscript x and quantities for a portion of the cross section with the subscript p. Flow depth for a portion of the cross section, h_p, is calculated by subtracting the bed elevation of that portion from the water surface elevation for the section as a whole, z_x. We used the resulting flow depths, h_p, and the section-average water surface slope, s_x, from equation (1) to compute mean daily velocity for each portion of the cross section using the Manning equation

$$U_p = \frac{h_p^{2/3} s_x^{1/2}}{n_x} \quad (2)$$

where U is mean streamwise velocity, n is the Manning's roughness coefficient. We obtained constant Manning's roughness values for each cross section from prior hydraulic calibrations of bathymetric data sets by USACE and CDWR. Next we calculated bed shear stress for each portion of a section, τ_p, as

$$\tau_p = \rho g h_p s_x \quad (3)$$

where ρ is the density of water and g is gravitational acceleration. In other words, we are making the approximation that all flow is parallel to the banks and bed. We converted shear stress to its dimensionless form [*Shields*, 1936]

$$\theta_p = \frac{\tau_p}{(\rho_S - \rho) g D_{50_x}} \quad (4)$$

where θ is dimensionless shear stress (i.e., Shields stress), ρ_S is density of sediment (assumed to be 2650 kg/m^3), and D_{50_x} is the characteristic (median) grain size of the bed material, obtained for each section from bulk material sampling. Lateral characterization of dimensionless shear stress (i.e., across the channel) could be improved by higher resolution bulk surveys of bed material, which would provide median grain size for each portion of the cross section, D_{50_p}. This may be particularly important in cases where there is marked lateral sorting of bed sediments (e.g., sections with coarse bars and fine-bedded pools).

6. Grain Size Groups

[16] Correct specification of sediment grain size is necessary in order to obtain realistic predictions of sediment flux because of the sensitivity of sediment transport equations to grain size distribution. For example, washload (i.e., that part of the sediment load which is not present on the riverbed) should not be computed with an equation designed to predict transport of bed material. The grain size range of a particular transport mode can be defined operationally as that which can be caught in a particular sampler [e.g., *Edwards and Glysson*, 1999]. The Helley-Smith bed load sampler [*Helley and Smith*, 1971] has been shown to be 100% effective in trapping grain sizes between 0.5 and 16 mm for a 75 mm intake (or 32 mm with a 150 mm intake) [*Emmett*, 1980], although difficulties may arise when it is used on uneven substrates. The DH-series, depth-integrated suspended sediment sampler is statistically effective at capturing sediment ranging from 0.001 to 0.5 mm in diameter [*Edwards and Glysson*, 1999], traveling more than 75 mm above the bed.

[17] We compared grain size distributions for bed material, suspended load, and bed load (for stations that had such data). These data show that 0.5 mm is an approximate lowest grain size for bed material at most stations in the basin. Bed material samples contain <5% of sediment finer than 0.5 mm, and sediment coarser than 0.5 mm constitutes <5% of all suspended samples. These factors indicate that 0.5 mm is the natural separation between washload and bed material load for mixed-bed reaches in the Sacramento basin. The sand-bed reaches at Butte City, Knights Landing, and Sacramento, have 0.25 mm as their lower limit (Figures 2c, 2e, and 2f). Suspended sediment is almost entirely comprised of washload in the Sacramento (Figure 2) and its tributaries, except at the Sacramento and Feather River stations (Figure 1), where significant quantities of fine-grained bed material move in suspension. However, for the remaining sections, there are two populations of sediment moving in distinct transport modes. Herein we model bed material discharge with the assumption that there is no overlap between them. We compute sediment discharge for up to nine grain size classes, subscript i, at each cross section. We use the geometric mean of each whole phi size class as our characteristic grain scale (i.e., D_{G_i} (mm) = 0.35, 0.71, 1.41, 2.83, 5.66, 11.31, 22.63, 45.25, and 90.51). At the lower end of the distribution (i.e., the smallest grain sizes), we limit the computations to grain sizes that constitute less than 5% of the suspended load at a given cross section. This is particularly important because we employ a sediment transport equation designed only for bed material transport calculations (see below). Note that we use the symbol D_{50_x} as the characteristic grain size for the whole bed material mixture and D_{G_i} as the characteristic size of each grain size class. D_{50_x} represents BMGSDs well because there are no strong bimodalities in the Sacramento bed material, although Butte City and Knights Landing are weakly bimodal (Figure 2).

7. Threshold Shear Stress

[18] Recent research in gravel transport has emphasized the importance of characterizing the threshold of incipient motion to ensure that sediment transport is not predicted in cases where the threshold for movement is not met. A more than threefold range in this threshold arises from the condition of the bed (e.g., grain shape, size, and packing, pocket angle). Numerous methods have been developed over eight decades of research [*Buffington and Montgomery*,

Table 1. Station Characteristics[a]

Station	Drainage Area, km^2	River Kilometer	Manning's n	WS Slope	D_{50_x}, mm	θ_{C_x}	Sort
Bend Bridge	23051	418.9	0.035	0.00131	17.00	0.070	2.362
Hamilton Cty	28645	320.7	0.035	0.00026	4.00	0.151	2.217
Butte Cty	31274	271.2	0.035	0.00050	4.00	0.184	2.368
Colusa	31313	231.1	0.035	0.00009	0.50	0.422	1.966
Knights Lndg	37645	144.2	0.035	0.00011	0.30	**0.422**	2.367
Sacramento	60886	96.0	0.030	0.00003	0.03	**0.422**	0.810
Cottonwood	2401	–	–	–	3.00	0.046	1.774
Cow	1101	–	–	–	9.00	0.123	2.875
Thomes	736	–	–	–	4.00	0.017	1.701
Feather	2065	–	–	–	0.30	**0.422**	0.479

[a]Station, drainage area, river kilometer, Manning's n, water surface slope (for baseline conditions), D_{50_x}, and θ_{C_x}, and sorting coefficient (sort). The bold values in the θ_{C_x} column represent stations for which no bed load data were available, and we applied θ_{C_x} from the nearest section with bed load data.

1997] to compute dimensionless critical shear stress, θ_{C_x}, and it is common practice to employ a characteristic value (e.g., θ_{C_x} = 0.03 [*Neill*, 1968], 0.047 [*Meyer-Peter and Muller*, 1948], 0.06 [*Shields*, 1936]) when local transport data are unavailable. In cases which bed load data are available, it is preferable to compute the local threshold value.

[19] This has been done commonly by a technique called similarity collapse originally developed in Japan [*Ashida and Michiue*, 1972; *Parker et al.*, 1982]. That method yields a power relationship with a coefficient that approximates the dimensionless critical shear stress, θ_{C_x}, for incipient motion of the entire mixture. However, the current study is not concerned with incipient motion of sediments. It is instead concerned with defining a threshold for sand and gravel transport that can be measured with a bed load sampler. This threshold is approximately 100 t/d for bed load data sets used herein (see below). Therefore we chose a θ_{C_x} that fits the minimum of this condition at each gauging station. In other words, we obtain θ_{C_x} by adjusting its value until excess shear stress (i.e., $\theta_x - \theta_{C_x}$) is positive for the hydraulic conditions corresponding to an observed transport rate near 100 t/d. This approach is especially useful to define a transport threshold in cases where a scarcity of bed load measurements leads to difficulties in defining the relationship between dimensionless transport and dimensionless shear stress. We recognize that this method may induce an upward bias in θ_{C_x} for stations where only high transport rates have been measured by Helley-Smith sampling. However, observed transport rates used to compute θ_{C_x} ranged from 76 to 172 t/d for all stations in the Sacramento valley, and from 76 to 104 t/d for all stations excluding Cow Creek. Table 1 provides information for each station including θ_{C_x}, drainage area, and median bed material grain size. For stations without bed load data (Knights Landing, Sacramento, and Feather River), we applied the θ_{C_x} from Colusa, where the BMGSDs and hydraulics were approximately similar to local conditions.

[20] The value of θ_{C_x} at Colusa (Table 1) is very high with respect to the range of incipient motion values reported in the literature [e.g., *Buffington and Montgomery*, 1997]. It describes a situation that has not been documented well in the literature. In a reach of river with artificial levees built upon channel banks, flow stages are elevated such that the river may adjust its bed slope and BMGSD to the prevailing flow conditions. In particular, flow energy otherwise expended on eroding natural banks may be focused into bed degradation, thus coarsening the bed and increasing bed slope. At the threshold condition for transport, increases in flow stage and water surface slope would outpace any increase in D_{50_x}, resulting in a higher θ_{C_x} value than would be computed for an unconstrained reach of similar dimensions (i.e., without flood control levees).

8. Sediment Transport Equation

[21] Previous researchers have computed sediment transport with formulae calibrated to specific laboratory and/or field data. Many such formulae have been extensively reviewed [e.g., *White et al.*, 1975; *Gomez and Church*, 1989]. The equations that *Gomez and Church* [1989] found to be most accurate (Bagnold and Parker et al.) were extensively calibrated on the best available measurements of bed load in gravel bed rivers. Most shear stress-based sediment transport equations are of a similar form [*Gomez and Church*, 1989], e.g., containing an excess shear stress term, or a ratio or difference of computed shear stress and critical shear stress raised to some power. Therefore we reason that it matters less which equation is used, but how well a particular equation can be calibrated to predict sediment transport in a particular river system. This is especially important because sediment transport computed with commonly-used equations may predict rates a factor of 2–10 times observed bed material transport rates, particularly for the highest recorded values. Until the theory of sediment transport improves to represent the range of laboratory flume and field sediment transport conditions, there is little utility in applying specific empirical equations to a new place without recalibrating to representative and/or local data, where they exist. Although such a practice has merit in studies investigating the applicability of particular equations [e.g., *Andrews*, 1981; *Batalla*, 1997], it has limited use in long-term prediction of sediment transport rates. Here we demonstrate that prediction of sediment transport rates in a particular place can be improved by calibrating a sediment transport equation of a commonly used form to local bed load and bed material data and simulating over a range of hydraulic conditions.

[22] Much of the following is loosely based on the derivation of a commonly used sediment transport equation for total load [*Engelund and Hansen*, 1967], which was developed by relating sediment transport to excess shear

stress and bed friction using data from flume experiments on a dune-covered sandy bed [*Guy et al.*, 1966]. We use the derivation of *Engelund and Hansen* [1967] as a guideline to develop a bed material transport equation appropriate for computing mass fluxes in mixed sediment beds with undeveloped (i.e., small, ill-defined) bed forms.

[23] We begin with a force balance between critical shear stress on the bed and the submerged weight of the sediment

$$\tau_C = \theta_C(\gamma_S - \gamma)D \tag{5}$$

where τ_C is critical shear stress, θ_C is dimensionless critical shear stress, γ_S is specific weight of sediment, γ is specific weight of water, and D is the characteristic grain size of the bed sediments. This equation represents the moment at which sediment movement begins.

[24] Next, following *Engelund and Hansen* [1967], we assume that sediment transport rate is proportional to the friction velocity in order to obtain

$$(\gamma_S - \gamma)q_{VBM}y = \alpha(\tau - \tau_C)LU_f \tag{6}$$

where $U_f = \sqrt{ghs}$, q_{VBM} is unit volumetric bed material load, y is bed form height, α is a dimensionless constant of proportionality, L is bed form length, and U_f is friction velocity. The left hand side is an expression of the gain in potential energy (per unit time and width) required to elevate the submerged sediment to a height y. The right hand side is the drag forces acting on the moving particles over length L during the same time interval. Rearranging, we get

$$fq_{VBM}\left(\frac{y}{fL}\right) = \alpha\frac{(\tau - \tau_C)}{(\gamma_S - \gamma)D}DU_f \tag{7}$$

where f is a friction factor (defined below). On the basis of flume observations, *Engelund and Hansen* [1967, p. 44] showed that alluvial beds adjust their bed to hydraulics in a dimensionless way. This is represented mathematically as

$$\left(\frac{y}{fL}\right) = const. \tag{8}$$

thus replacing the explicit description of bed forms and form drag with an implicit representation of their effects within the alpha parameter (e.g., as a drag coefficient). We acknowledge that the formulation in equation (8) does not account for form drag associated bar-scale bed undulations and river curvature, which induce flow expansion/contraction, etc. and generally consume flow energy. These factors will also be included in the alpha parameter.

[25] Next we define

$$f = \frac{2ghs}{U^2} \tag{9}$$

and

$$\theta = \frac{\tau}{(\gamma_S - \gamma)D} = \frac{U_f^2}{\left(\frac{\gamma_S}{\gamma} - 1\right)D} \tag{10}$$

to obtain

$$q_{VBM} = \alpha\frac{U^2(\theta - \theta_C)\sqrt{\theta}\sqrt{\left(\frac{\rho_S}{\rho} - 1\right)gD^3}}{2ghs} \tag{11}$$

[26] This generalized form of our sediment transport equation is nearly identical to an unnumbered equation in *Engelund and Hansen* [1967, p. 48], before they specify a value of θ_C and calibrate the equation to flume data [*Guy et al.*, 1966]. We now make a few modifications to (11) to arrive at a fractional mass flux bed material load equation that is sensitive to properties of the bed material and useful for making transport calculations for particular portions of a river channel.

[27] First, we multiply equation (11) by sediment density to obtain a mass flux equation. Second, we compute flux for individual portions of the channel (subscript p) using hydraulic variables for each portion. Third, we compute bed material flux for each grain size class (i.e., fractional load) by specifying a characteristic grain size for the grain class of interest, i, and multiplying the right-hand-side of equation (11) by the fraction of the bed material in that class. Fourth, to make the computations specific to transport in a particular grain size class, we replace the Shields stress under the square root sign with Shields stress computed for the characteristic grain diameter of the grain size class of interest. In other words, we are computing fractional transport specific to the shear stress of a particular particle size once the whole bed mixture has reached the previously defined threshold (i.e., once the excess shear stress term is positive). It deserves repeating here that we are not concerned with incipient motion, but with a threshold of transport when gravel and sand are in motion. In other words, we are not assuming equal mobility during incipient motion [e.g., *Parker et al.*, 1982]. These changes result in

$$q_{BM_{pi}} = \alpha\frac{\rho_S U_p^2(\theta_p - \theta_{C_x})\sqrt{\theta_{pi}}\sqrt{\left(\frac{\rho_S}{\rho} - 1\right)gD_{G_{x_i}}^3}}{2gh_p s_x}F_{x_i} \tag{12}$$

where $q_{BM_{pi}}$ is the unit bed material transport rate in kg/s per m of width in portion p of the cross section of size class i, θ_p is dimensionless shear stress computed for h_p and DG_x, θ_{C_x} is the dimensionless critical shear stress for the whole mixture, θ_{pi} is dimensionless shear stress computed for a particle in size class i, and F is the fraction of bed material in a particular grain size class. Equation (12) is dimensionally homogenous and may be used with any set of units.

9. Calibration

[28] We sought to develop a calibrated equation that could predict sediment transport of any grain size class and at any cross section within the Sacramento basin. High flux rates of bed material are our main concern because of the general experience that the majority of a river's sediment is transported by a few high flows [*Lustig*, 1965; *Stewart and LaMarche*, 1967; *Pitlick*, 1988]. Therefore we have calibrated alpha only to bed load

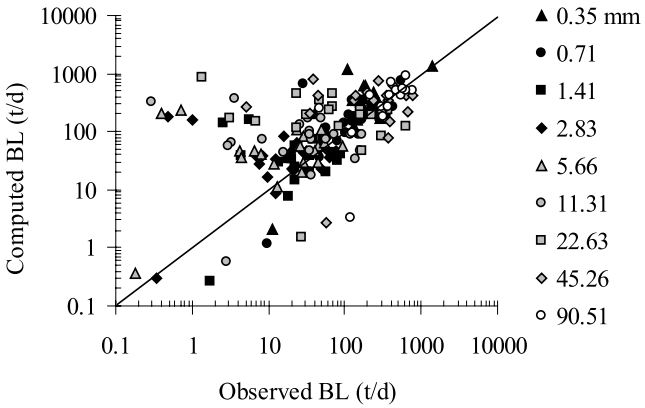

Figure 4. Plot of computed bed load versus observed bed load for Snake River, Idaho, using equation (12) calibrated to data in each grain size class. Calibrations were restricted to total transport rates (sum of all transported grain sizes) greater than 100 t/d.

measurements greater than 100 t/d (e.g., a condition in which both sand and gravel are measured in transport). This will improve the prediction of sediment transport during the highest flood peaks and our overall estimation of long-term bed material flux, and is consistent with our computation of θ_{C_x} (see above). Our stochastic flow model, HYDROCARLO, was designed to simulate flow above a flood threshold (Singer and Dunne, submitted manuscript, 2003), in order to model the effect of large events on, among other things, bed material flux.

[29] However, ample main stem bed load data (e.g., at least 5 measurements greater than 100 t/d) for calibration were not available for Sacramento River gauging stations. Therefore we calibrated (12) using bed load data from a range of other representative fluvial environments by adjusting the α parameter for each grain size class (i.e., including all fractions present in the bed material, but not significantly represented in suspended samples, Figure 2) to achieve the best fit between computed and measured transport rates. We used Helley-Smith bed load data from Clearwater and Snake Rivers in Idaho and the Tanana River in Alaska, which were publicly available [*Emmett and Seitz*, 1973, 1974; *Jones and Seitz*, 1979, 1980; *Burrows et al.*, 1981; *Harrold and Burrows*, 1983] and represent the range of mixed bed conditions found along the Sacramento. Figure 4 shows the ability of equation (12) to predict fractional sediment transport for bed load data from the Snake River in Idaho. Generally predictions fall within a factor of two of observed values, although a few large discrepancies are apparent. Given the stochasticity in the driving factors of sediment transport, the stochasticity in transport itself, and the operational limits to its measurement, Figure 4 is reasonably encouraging. However, more systematic data sets for calibration would be useful to define the limits of equation (12).

[30] Figure 5 shows our fitted α values plotted against grain size for three data sets. It is apparent from this plot that fitted α values show a relationship with grain size. Although α contains implicit description of river bed forms, we reason that α is primarily a function of BMGSDs. We analyzed fitted α values for the various data sets and determined that superposition of the α curves in Figure 5 can be explained as a function of bed material sorting and grain particle hiding:

$$\alpha = \alpha\left(\sigma_\phi, \frac{D_{G_{x_i}}}{D_{50_x}}\right) \tag{13}$$

[31] Sorting is sedimentological parlance for the "spread" or logarithmic standard deviation of a grain size distribution. The sorting coefficient of the bed material, σ_ϕ, first presented by [*Krumbein*, 1938], describes the sorting of the bed. High values of sorting signify a large standard deviation and vice versa. For each river used in the calibration of (12), we computed bed material sorting (phi scale) of grains falling between 0.25 mm and 128 mm by the method of moments within GRADISTAT, a grain size analysis software package [*Blott and Pye*, 2001].

[32] Hiding is a concept formalized by *Einstein* [1950] and later modified by *Egiazaroff* [1965] to account for larger drag forces on grains that protrude into the flow. Therefore protrusion of a grain above its neighboring grains increases its mobility over that which would be expected based on its weight alone. Likewise, small grains get hidden, reducing their mobility. Hiding can be assumed to operate on a grain of a particular size relative to the median grain size of the bed.

[33] We developed a multiple regression model for alpha as a function of grain size and bed material sorting (adjusted $R^2 = 0.92$, n = 26):

$$log_{10}\alpha = 1.62{*}\sigma_\phi + 0.58{*}\left(\frac{D_{G_i}}{D_{50_x}}\right)^{-0.5} - 7.85 \tag{14}$$

We use a power function of hiding with an exponent iteratively selected for the best fit in equation (14). The resulting hiding function exponent, -0.5, is similar to two reported values (i.e., -0.56 [*Wathen et al.*, 1995] and -0.65 [*Komar*, 1987]), which suggest a deviation from the strong form of the equal mobility hypothesis [*Parker and Toro-Escobar*, 2002]. We tested model assumptions of (14) by assessing the normality and randomness of the standardized residuals and it passed both. Figure 5 suggests that the value of alpha has a lower limit of $\sim$0.0001 for the three data sets

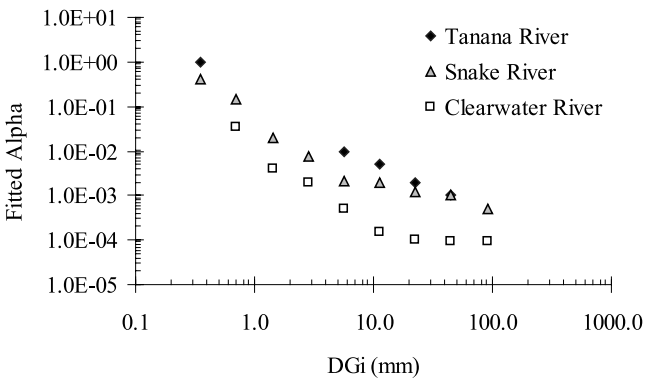

Figure 5. Fitted alpha (coefficient in equation (12)) values from calibrations to bed load data in each grain size class. We restricted calibration to total transport rates greater than 100 t/d.

used herein, which is consistent with recent understanding of how beds of a narrow range of grain sizes with limited sediment supply can form close packings that are difficult to mobilize [e.g., *Church and Hassan*, 2002]. Although a detailed assessment of the range of applicability of (14) is beyond the scope of this study, the equation appears appropriate for the range of bed conditions found in the Sacramento. Equation (14) was used to determine alpha for each grain size for each Sacramento cross section according to its bed material properties.

10. Daily Bed Material Flux Simulation and Total Load Evaluation

[34] To summarize our method, we ran HEC-RAS driven by fifty, 30-year HYDROCARLO streamflow simulations through topographic cross sections from a DEM, and used the stage output at six cross sections with equations (1), (2), (3), (4), and (12) to obtain daily sediment transport estimates for each grain size class in each portion of a cross section. Computations of fractional bed material flux incorporate local hydraulics, local threshold shear stress, and calibrations of equation (12) to local BMGSDs (based on the relationship in equation (14) developed for alpha from extra-Sacramento data sets from a range of fluvial environments). We computed bed material flux for each grain size class multiplied by its percentage in the bed material (excluding surface armor).

[35] For simplicity, we also assumed one-dimensional flow, no armoring of the bed surface, and no cross-sectional change, all of which could be relaxed in later iterations of the model. Beyond the percentages of each grain size class present in the bed material, we place no limits (e.g., armoring, scour depth) on sediment supply as transport rates increase in the current version of this method. Armoring of the river bed due to selective transport of small grain sizes increases the median grain size and increases sorting (decreases the sorting coefficient, or standard deviation of grain sizes), resulting in less sediment transport. Scour of bed sediments during flood events generally occurs only down to a depth limited by local geology and grain sizes at this depth. Therefore sediment transport during a flood event can occur only until the scour depth is reached, at which point it would shut off. Although these effects may affect bed material transport, there are currently no data for assessing their influence in the Sacramento. Consequently, we have not as yet incorporated armoring and scour depth into the modeling method.

[36] We computed daily bed material loads in each size class for the entire cross section as

$$Q_{BMDay_{x_i}} = \sum_p q_{BM_{p_i}} w_p * 86400 \sec . \quad (15)$$

where $Q_{BMDay_{xi}}$ is daily bed material transport and w_p is the width of a particular portion of the cross section. Next, we computed annual average sediment load for each simulation

$$Q_{BMYear_{x_i}} = \frac{\sum_{Day} Q_{BMDay_{x_i}}}{t} \quad (16)$$

where $Q_{BMYear_{xi}}$ is annual total bed material load and t is the number of years in each simulation. Finally, from the values

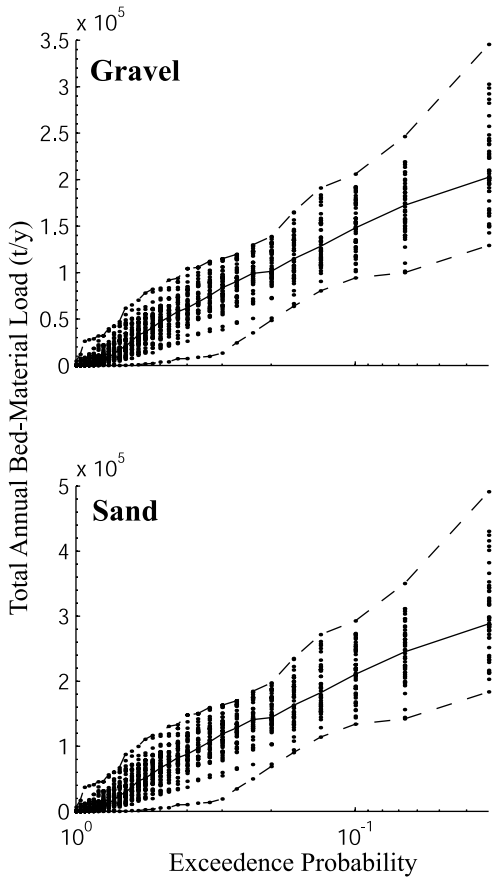

Figure 6. Total annual bed material loads (t/y) for (top) gravel and (bottom) sand at Hamilton City plotted against exceedence probability. The median of all simulations is represented by the solid line and the extrema by dashed lines.

produced by equation (16), we calculated the annual transport extrema (i.e., maximum and minimum) and median for all simulations. Thus our method results in estimates of central tendency, as well as variability in transport prediction, based on stochastic hydrology.

[37] It is important to distinguish our method from one that seeks to characterize measurement or modeling uncertainty [e.g., *Wilcock*, 2001]. Our method uses the variability in the flow regime to define the range and probability distribution of sediment flux to be expected from the variable flow (and ultimately precipitation). We have minimized the uncertainty in hydrology by modeling it (Singer and Dunne, submitted manuscript, 2003). However, we have made no assessment of uncertainty associated with measurement or parameter specification. The error bars around an estimate therefore are not estimates of uncertainty; they are descriptions of variability due to flow. For example, the range at 50% exceedence probability is a measure of the variance in the estimate of the median exceedence.

[38] Figure 6 shows annual total bed material load in tons/year plotted against exceedence probability for gravel and sand at one main stem station (Hamilton City, Figure 1). For example, our simulations show that in about 50% of years annual total gravel transport at Hamilton City exceeds a value that ranges between 3000 and 83,000 t/y with a

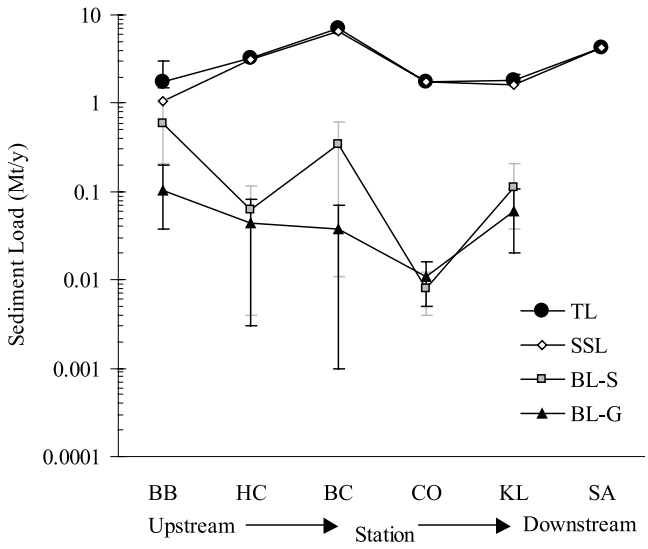

Figure 7. Main stem median annual sediment loads (Mt/y) including total load (TL), suspended load (SSL), sand bed material load (BL-S), and gravel bed material load (BL-G). Suspended loads were simulated in a previous study [*Singer and Dunne*, 2001]. The error bars on the bed material estimates represent the variability associated with stochastic hydrology. Gravel bed material load ranges from 0 to 6% of total load.

median of ~44,000 t/y. Such an annual load is equivalent to the transport of a volume of bed material 200 m wide (the average channel width) multiplied by a sediment bulk density of 1.8 t/m^3 and an average particle travel distance of 800 m/y (the average annual transport distance of gravel tracers in the Sacramento River [*California Department of Water Resources*, 1992]), and an average scour depth of ~0.15 m. This scour depth is equivalent to 6 times the grain diameter of D_{90_s} (Figure 2b).

[39] In the following paragraphs we present transport results for each main stem gauging station based on similar simulations. In the subsequent section, we use these transport estimates and those from tributaries to evaluate net changes in storage in the reaches of river between each main stem gauging station.

[40] Figure 7 shows the results of gravel and sand bed material transport for our simulations at all main stem cross sections. We have also plotted suspended load simulated from our previous analysis [*Singer and Dunne*, 2001] and total load obtained by summing sandy bed material load, gravelly bed material load, and suspended (predominantly silt) loads. The method predicts that gravel transport makes up anywhere from 0 to 6% of total load depending on the station, which is an expectable range.

[41] The method presented for computing bed material load produces transport patterns similar to those obtained for suspended sediment transport modeling [*Singer and Dunne*, 2001] based on time series analysis of historical USGS sampling (discharge and sediment concentration), providing some other circumstantial evidence in support of the calculated bed material transport. A direct comparison of bed material and suspended loads computed via HYDROCARLO is beyond the scope of this study. Nevertheless, both bed material and suspended load transport studies predict an increase in fine sediment transport between Hamilton City (HC) and Butte City (BC). It appears that the predicted increase in sandy bed material transport is, at least in part, due to a decrease in coarse sediments and an increase of medium sand in the bed material at BC (Figure 2). This change in bed material probably arises because the Sacramento River downstream of HC is no longer in contact with Pleistocene river gravels, which supply bank material from upstream (Red Bluff formation in 1:250,000 Calif. Division of Mines and Geol. quadrangles). Our bed material method also predicts a decrease in sand and gravel bed material load between Butte City (BC) and Colusa (CO), which is consistent with the dramatic simulated reduction in suspended sediment load [*Singer and Dunne*, 2001]. Colusa marks a transition in transport pattern, where a major deflection of the river eastward around the Colusa Dome and localized movement on the Willows fault [*Harwood and Helley*, 1987], lowers the channel gradient, forces decanting of washload into Sutter Bypass [*Singer and Dunne*, 2001], and deposition of sediments in the wide upstream reach of valley.

[42] In other locations, predicted bed material transport patterns diverge from their suspended load counterparts. The bed material method predicts a decrease in transport between BB and HC (Figure 7), which probably reflects the increase in valley width associated with the Sacramento's transition from an entrenched river in Iron Canyon to an aggraded, lowland river in the Central Valley. The valley width increase allows for more in-channel accommodation space, where bed sediments can organize into weak bed forms, perhaps resulting in better sorting of the bed material mixture (i.e., lower sorting coefficient, Table 1) and finer bed material at HC (Figure 2). The computations point to a slight decrease in gravel transport between HC and BC that is due to less gravel in the bed material at BC, suggesting gravel deposition in reach 2.

[43] Transport calculations also show an increase in bed material load between CO and KL (Figure 7), which is consistent with the observation of an abrupt increase in 8–32 mm gravels and medium sand in the bed material at Knights Landing (Figure 2). These factors suggest that there is a sediment source in reach 4. Inspection of the Sacramento geologic quadrangle (1:250,000, California Divison of Mines and Geology) reveals that the Sacramento River is dissecting unconsolidated Pleistocene fanglomerates of Cache Creek, which extend across the floodplain in reach 4. The local change in bed material results in a relatively high sorting coefficient (Table 1) and thus high bed material transport. Finally, bed material calculations predict no bed material load at Sacramento (SA) and thus huge declines in transport between KL and SA. This result stems from an extremely low sorting coefficient at SA (Table 1), minute quantities gravel in the bed material (Figure 2f), and low (or occasionally negative) water surface slopes at this section, which is located in the tidal zone. These factors do not, however, appear to influence suspended load, which increases at Sacramento probably because of fine sediment delivery from the Feather and American Rivers (tributaries shown in Figure 1). However, given observations of dune bed forms in this reach (our unpublished observations from

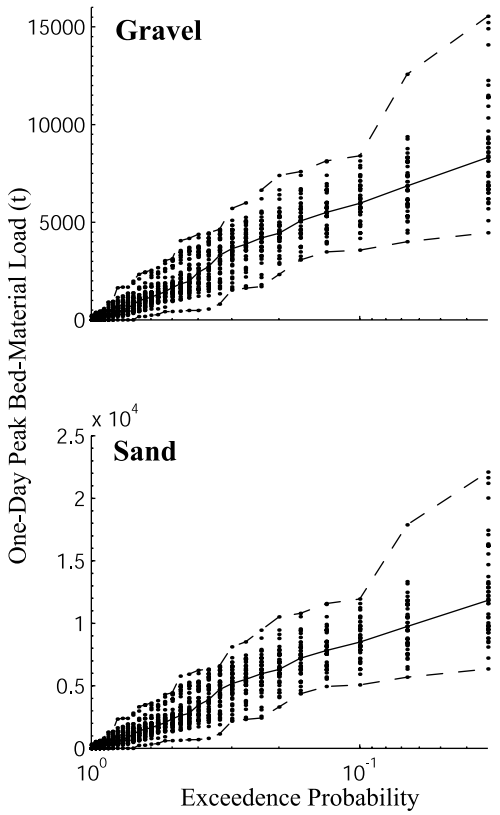

Figure 8. One-day peak bed material loads (t) for (top) gravel and (bottom) sand at Hamilton City plotted against exceedence probability. The median of all simulations is represented by the solid line and the extrema by dashed lines.

depth sounding and those of R. Dinehart, USGS, personal communication), it is likely that sandy bed material is being transported along the bed as sand waves (not represented in our model).

[44] We also calculated annual one-day peaks in bed material load for each simulated year to ascertain the role of individual flood events on sediment transport. As before, median and extrema of this value, for a given exceedence probability, are determined for the 30 simulations (Figure 8). The highest one-day sand transport peak for all simulations is ~22,000 t, or ~35% of the median annual total sand flux at Hamilton City. Annual totals and one-day peaks of bed material transport will be used in the next section to evaluate net changes in reach-averaged sediment storage.

11. Bed Material Budgets

[45] We evaluated simple main stem sediment budgets from the estimates of total annual bed material load into the Sacramento from tributaries and the changes in load between each main stem gauging station. These are crude mass balances in the sense that we compute how much sediment gets stored in or eroded from a given reach, but we provide no mechanistic explanation of how the mass balance is being struck within the reach (e.g., changes in morphology or bed elevation patterns).

[46] We computed bed material influx to the Sacramento River from four signature tributaries, which represent the four geologic provinces used by *Singer and Dunne* [2001]. Tributary loads were also computed by driving equation (12) with discharge simulated by HYDROCARLO [*Singer and Dunne*, 2001]. However, instead of routing this flow with HEC-RAS, we obtained mean flow depths, h_x, for each day from stage-discharge rating curves at the USGS gauges. Since we had no calibrated values of Manning's n to compute velocity in equation (2), we constructed a velocity-stage rating curve from USGS current meter measurements. We measured slopes from USGS 7.5-minute topographic quadrangles for use in equation (3). BMGSDs were available for each tributary station. As in the suspended load study, we scaled the computed signature tributary loads (and their uncertainties) by the ratio of drainage areas to compute the load entering the main stem from each Sacramento tributary. We combined the time varying tributary loads with those computed for main stem stations to evaluate reach-averaged, bed material budgets.

[47] We recognize the shortcomings of scaled bed material loads (e.g., deposition of bed material load upstream of confluence with the main stem), but inspection of aerial photographs for each tributary reach revealed no obvious zones of erosion/deposition in the short reaches between the most downstream gauge and the confluence with the main stem. Further, since the Sacramento River flows in the central part of its valley, tributaries must cross a substantial part of this valley before their confluence with the main stem. We argue that since slope in these distal tributaries reaches is fairly uniform across tributary basins, bed material loads may be reasonably scaled by drainage area.

12. Annual Total Bed Material Load

[48] We computed the budgets for annual total bed material load, which indicates long-term spatial patterns in main stem sediment transport. Annual divergence, or net difference in bed material load, was computed for each reach as

$$\Delta Q_{BMYear_R} = Q_{BMYear_{Up}} - Q_{BMYear_{Down}} + Q_{BMYear_{Tribs}} \quad (17)$$

where ΔQ_{BMYear_R} is reach-averaged (R) change in annual (Y) total bed material load; Q_{BMYear} is annual total bed material load, and the subscripts *Up*, *Down*, and *Tribs*, indicate the upstream, downstream and tributary locations, respectively. We assume that no bed material load leaves the reach through flood diversions, which decant mostly washload [*Singer and Dunne*, 2001], and that fining by attrition is negligible. This type of budget may be computed for each grain size (because we compute fractional transport rates), but for simplicity we present results from budgets computed for total bed material load, sand load, and gravel load in Figure 9. The computational spreadsheets for annual gravel and sand bed material load are contained in Supporting Material A and B.

[49] The bars in Figure 9 represent the median of the expected range (i.e., the 50% exceedence probability) of net erosion or deposition for a year and for a reach, and the T-bars represent the extrema of this range resulting from all simulations of stochastic hydrology (i.e., fifty 30-year runs). The T bars increase in magnitude in the downstream direction because we propagated the variability. The upper T bars, for example, represent the maximum of the expected range (i.e., the 50% exceedence probability) for all upstream

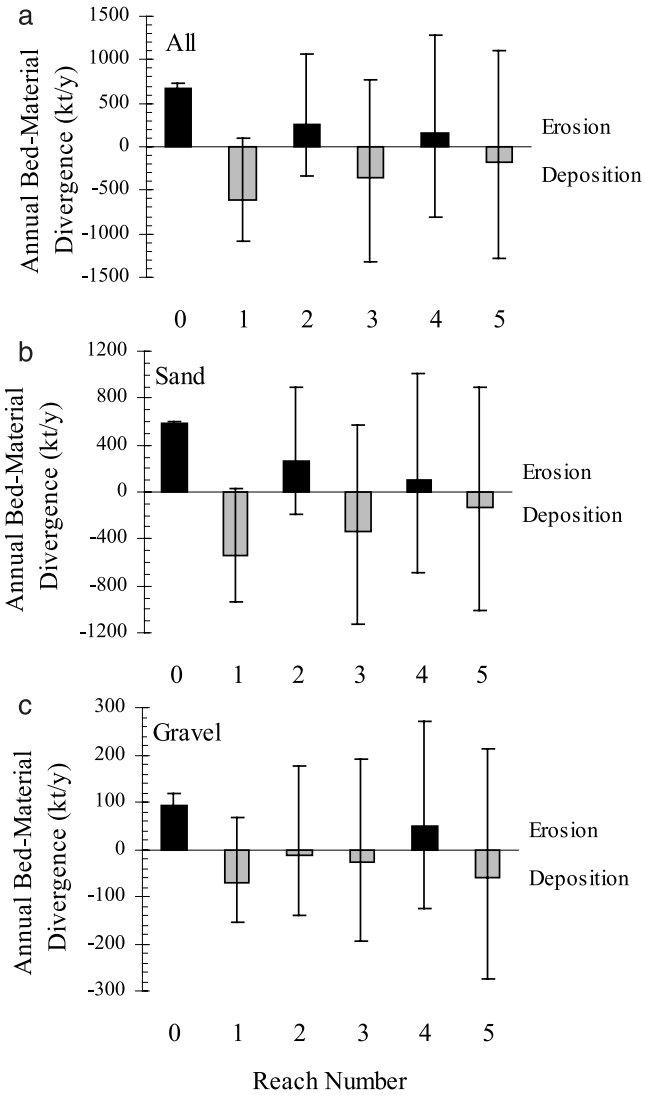

Figure 9. Total annual bed material budgets for all bed material, sand portion, and the gravel portion. Divergences (kt/y) are net differences in sediment transport for each reach. Negative divergence is deposition and positive is erosion. Error bars represent the variability in the annual total divergences associated with stochastic hydrology, which was propagated downstream.

main stem stations and tributaries added together. The lower T bars represent the same for the minimum of the range. They represent the capacity for the short-term imbalances in total reach sediment storage.

[50] Our previous work has shown that large frontal storms frequently affect the whole of the Sacramento basin, inducing floods of similar relative magnitude at distant ends of the basin (Singer and Dunne, submitted manuscript, 2003). Therefore it is possible (however unlikely) to record the most extreme flood at all gauges in the tributary network and thus a sum of upstream extrema bed material flux past main stem gauging sites. We have not yet analyzed hydroclimatology in the Sacramento valley in detail, and may eventually make modifications to our simplified propagation of variance based on such studies.

[51] The budget for annual total bed material load indicates significant net bed material erosion in reaches 0, 2, and 4, and deposition in reaches 1, 3, and 5 (Figure 1). We compared this budget with one previously evaluated for suspended load [*Singer and Dunne*, 2001, Figure 6], which identified erosion in reaches 2, 4, and 5 and net deposition in reaches 0, 1, and 3. reaches 1, 2, 3, and 4 show a similar pattern in both budgets, indicating similarities in storage patterns between the various modes of sediment transport except at the upper and lower ends of this study. It should be noted that the suspended load budget was evaluated using historical flow and sediment samples, because the time series approach used in that study does not lend itself to simulation under a range of flow conditions. It is worth clarifying here that in light of the data in Figure 2, we have determined that calculations of deposition and erosion of suspended sediment in our previous study [*Singer and Dunne*, 2001] primarily describe washload storage in and mobilization from banks, as opposed to erosion from the bed. An explanation of the differences between the bed material load and suspended load budgets requires a better understanding of the sources of and the controls on washload in the Sacramento basin, so the following discussion will be mostly limited to the simulated bed material budgets.

[52] Figures 9b and 9c show annual total budgets for sand and gravel, respectively. These budgets are subsets of Figure 9a that reveal which grain size fractions are responsible for the net divergence in a given reach. The majority of the simulated divergences result from imbalances in sand bed material transport, as one would expect. However, significant gravel divergences can indicate the state of the riverbed in a given reach. For example, gravel erosion is predicted in reaches 0 and 4. Erosion of gravels predicted in reach 0 is unsurprising for a mixed bed of sand, gravel, and bedrock in a relatively steep (Table 1), narrow canyon. Additionally, Shasta Dam controls reach 0 at its upstream end, so we have assumed no sediment input from upstream, $Q_{BMYear_{Up}}$. The predicted erosion is due to hungry water below the dam, which has coarsened the bed, despite sediment delivery from tributaries in reach 0. Annual gravel erosion in reach 0 is predicted to be ~2 cm/y, or approximately the diameter of D_{50_x} at BB (Figure 2a), when averaged over the area of the bed in that reach, assuming a transporting width of 75 m (since half of the reach is bedrock). With no additional upstream sources of gravel entering the reach (i.e., beyond the simulated tributary input), net erosion and coarsening in this reach is predicted to prevail. Recent augmentation of 20–60 mm spawning gravel in reach 0 by CDWR [*California Department of Water Resources*, 1980] corroborates this conclusion. However, our methods have not directly accounted for reduced transport due to armoring of the bed surface.

[53] Annual predicted gravel erosion rate in reach 4 is 0.3 cm/y, which corresponds to the diameter of D_{50_x} at KL. As previously discussed, this erosion likely results from the dissection of a Pleistocene fan composed of fine and medium size gravels. An increase in gravel transport seems reasonable in a locale where a local source of gravel can be transported over an increasingly sandy bed (Figure 2). It is unclear when the Sacramento River will exhaust the supply of gravel from the portion of the fan that is being accessed by the leveed reach 4.

[54] Significant sand erosion is predicted in reaches 0, 2, and 4. In a fashion similar to that for gravel, sand erosion in reach 0 is primarily a function of sediment starvation by the dam upstream. Erosion of sands in reaches 2 and 4 is probably due to a shift in grain sizes in suspension. Figures 2b, 2c, 2d, and 2e show the suspended load fines between HC and BC, and between CO and KL. The 0.35 mm fraction of the suspended load decreases from 6% to 3% between HC and BC and from 8% to 2% between CO and KL, in favor of finer particle sizes. There are concomitant increases of that fraction in the bed material (from 1% to 12% between HC and BC and from 19% to 32% between CO and KL). Our modeling of suspended load [*Singer and Dunne*, 2001] concluded that net erosion of suspended load prevails between HC and BC and between CO and KL (probably as bank erosion). As banks are eroded, fine sediment in silty banks is mobilized in suspension and sandy fractions are added to the bed. It is likely that bank erosion is the primary source of sediment that fines the suspended load and the bed material, contributing to high rates of sand transport past the Butte City and Knights Landing and thus net sand erosion in these reaches (Figure 9b).

[55] The deposition of both sand and gravel in reach 3 probably results from the reduction of flood discharge by diversion of water into the flood bypass above Colusa as previously discussed. Deposition in reach 5 is the combined effect of large sand loads into this reach from the Feather River and significant fine gravel loads entering from upstream. It appears that reach 5 is a sink for gravel that gets buried (Figure 2f) by two times more sandy bed material deposition than gravel.

13. Discussion and Conclusion

[56] We have developed a method for simulating daily bed material flux in the Sacramento River channel system, but it cannot yet be tested empirically because the necessary measurements do not exist. To reduce sources of uncertainty not associated with stochastic hydrology, we have tried to accurately parameterize each equation based on the best available data sets of channel dimensions, hydraulic data, bed material texture, and bed load transport. We have made no attempt herein to analyze the sensitivity of the results to any particular parameter, which is beyond the scope of the current study. However, it is clear that specification of alpha (i.e., a function of sorting and hiding) plays a significant role in determining transport for a given set of hydraulic conditions.

[57] The accuracy of transport predictions (and budgets) can be improved for a particular basin by collecting more field data. Although the Sacramento is a data-rich basin, every basin lacks some data necessary for making accurate decadal sediment transport estimates. This situation, combined with the desire to simulate the influence of a range of yet unrecorded hydrologic conditions, necessitates modeling of the variety presented herein. Increased data collection efforts can provide the basis for testing a given model and (ultimately) for improving model predictions.

[58] We have already discussed the need for assessing armoring and scour depth, but there are other data collection opportunities that would improve this method. For example, simulations on the Sacramento would benefit from bed load measurements and bed material surveys for each major tributary to simulate influx from each separately, instead of scaling loads from signature tributaries. Additional cross sections could also be surveyed in tributary basins so that explicit flood routing could be conducted to obtain water surface profiles for use in equation (2), and to calibrate Manning's n for use in equation (3). Bed load flux measurements for Knights Landing, Sacramento, Feather River, and other sandy environments would also be useful to determine θ_C for these stations and to improve transport calibrations for sand-bed rivers. Recent and consistent bed material samples are required to accurately characterize grain size distributions at all stations. Finally, more bed load data from a wider range of fluvial environments would improve calibration of equation (14).

[59] The alpha parameter is estimated as a function of two properties of the bed material: the sorting coefficient and the hiding function. The inclusion of these two properties in the multiple regression in (14), results in a high value of R^2, and there are reasons to believe that the improvement in prediction results from incorporation of first order sedimentary controls on bed material mobility. Various studies have recently stressed the importance of BMGSDs on critical shear stress, and especially the variability in pocket geometry and packing that lead to a wide distribution in critical shear stress [e.g., *Wiberg and Smith*, 1987; *Kirchner et al.*, 1990]. In particular, *Kirchner et al.* [1990] outlined a scenario of a varying threshold for transport that induces large variability in transport rates. In our calibration of alpha, we have represented an analog to this scenario, wherein the threshold is fixed, but transport rates vary according to bed conditions. We hypothesize that the combination of sorting and a hiding function is a first order descriptor of pocket geometry and packing. This hypothesis is consistent with field data demonstrating high sediment transport rates in very poorly sorted materials [*Burrows et al.*, 1981; *Harrold and Burrows*, 1983; *Paola and Seal*, 1995; *Reid and Laronne*, 1995]. A systematic calibration of an equation like equation (14) to more bed load data sets from a variety of large river environments is suggested.

[60] The method introduced here simulates sediment flux associated with flood days above a threshold. This threshold was developed by a repeatable statistical procedure (Singer and Dunne, submitted manuscript, 2003), without consideration of thresholds for sediment transport, for instance. This is because HYDROCARLO was designed to simulate flows at the upper, less frequent end of the flood frequency curve. We have demonstrated how our method of basinwide sediment flux simulation may be applied to sediment budgets, but it may also be useful in predicting channel geometry resulting from an integration of rare, large flows over a period of years or decades. It has further potential to aid in the design and implementation of river rehabilitation strategies (e.g., gravel augmentation), which generally require a prediction horizon of decades and a characterization of risk.

[61] **Acknowledgments.** We acknowledge the helpful comments of Tom Lisle and an anonymous reviewer, which greatly improved the manuscript. We thank Tanya Ehorn and Koll Buer at CDWR for data provision and Gary Parker for comments and suggestions on sediment transport computations. We acknowledge support from CALFED grant 4600002659 and NASA grant NAG5-8396.

References

Andrews, E. D. (1981), Measurement and computation of bed-material discharge in a shallow sand-bed stream, Muddy Creek, Wyoming, *Water Resour. Res.*, *17*(1), 131–141.

Ashida, K., and M. Michiue (1972), Study on hydraulic resistance and bedload transport rate in alluvial streams, *Trans. Jpn. Soc. Civ. Eng.*, *206*, 59–69.

Batalla, R. J. (1997), Evaluating bed-material transport equations using field measurements in a sandy gravel-bed stream, Arbucies River, NE Spain, *Earth Surf. Processes Landforms*, *22*, 121–130.

Blott, S. J., and K. Pye (2001), Gradistat: A grain size distribution and statistics package for the analysis of unconsolidated grains, *Earth Surf. Processes Landforms*, *26*, 1237–1248.

Buffington, J. M., and D. R. Montgomery (1997), A systematic analysis of eight decades of incipient motion studies with special reference to gravel-bedded rivers, *Water Resour. Res.*, *33*(8), 1993–2029.

Burrows, R. L., W. W. Emmett, and B. Parks (1981), Sediment transport in the Tanana River near Fairbanks, Alaska, 1977–79, *U.S. Geol. Surv. Water Resour. Invest. Rep.*, *81–20*, 56 pp.

California Department of Water Resources (1980), Upper Sacramento River spawning gravel study, Red Bluff, Calif.

California Department of Water Resources (1992), Sacramento River spawning gravel restoration phase I progress report, 37 pp., Red Bluff, Calif.

Church, M., and M. A. Hassan (2002), Mobility of bed material in Harris Creek, *Water Resour. Res.*, *38*(11), 1237, doi:10.1029/2001WR000753.

Dunne, T., L. Mertes, R. Meade, and J. Richey (1998), Exchanges of sediment between the flood plain and channel of the Amazon River in Brazil, *Geol. Soc. Am. Bull.*, *110*(4), 450–467.

Edwards, T. K., and G. D. Glysson (1999), Field methods for measurement of fluvial sediment, *U.S. Geol. Surv. Tech. Water Resour. Invest.*, *Book 3*, Chap. C2.

Egiazaroff, I. V. (1965), Calculation of non-uniform sediment concentrations, *J. Hydrol. Eng.*, *91*(4), 225–248.

Einstein, H. A. (1950), The bed load function for sediment transportation in open channels, *Tech. Bull. 1026*, Soil Conserv. Serv., U.S. Dep. of Agric., Washington, D. C.

Emmett, W. W. (1980), A field calibration of the sediment-trapping characteristics of the Helley-Smith bedload sampler, *U. S. Geol. Surv. Prof.*, *1139*.

Emmett, W. W., and H. R. Seitz (1973), Suspended- and bedload-sediment transport in the Snake and Clearwater Rivers in the vicinity of Lewiston, Idaho, March, 1972 through June, 1973, report, U.S. Geol. Surv., Reston, Va.

Emmett, W. W., and H. R. Seitz (1974), Suspended- and bedload-sediment transport in the Snake and Clearwater Rivers in the vicinity of Lewiston, Idaho: July, 1973 through July, 1974, report, U.S. Geol. Surv., Reston, Va.

Engelund, F., and E. Hansen (1967), *A Monograph on Sediment Transport in Alluvial Streams*, 63 pp., Teknisk Vorlag, Copenhagen.

Gomez, B., and M. Church (1989), An assessment of bed load sediment transport formulae for gravel bed rivers, *Water Resour. Res.*, *25*(6), 1161–1186.

Guy, H. P., D. B. Simons, and E. V. Richardson (1966), Summary of alluvial channel data from flume experiments, 1956–61, *U.S. Geol. Surv. Prof. Pap.*, *462-I*.

Harrold, P. E., and R. L. Burrows (1983), Sediment transport in the Tanana River near Fairbanks, Alaska, 1982, *U.S. Geol. Surv. Water Resour. Invest. Rep.*, *83-4213*.

Harwood, D. S., and E. J. Helley (1987), Late Cenozoic tectonism of the Sacramento Valley, California, *U.S. Geol. Surv. Prof. Pap.*, *1359*.

Helley, E. J., and W. Smith (1971), Development and calibration of a pressure-difference bedload sampler, open file report, 18 pp., U.S. Geol. Surv., Reston, Va.

Jones, M. L., and H. R. Seitz (1979), Suspended- and bedload-sediment transport in the Snake and Clearwater Rivers in the vicinity of Lewiston, Idaho, August 1976 through July 1978, *U.S.Geol. Surv. Open File Rep.*, *79-417*, 87 pp.

Jones, M. L., and H. R. Seitz (1980), Sediment transport in the Snake and Clearwater Rivers in the vicinity of Lewiston, Idaho, *U.S. Geol. Surv. Open File Rep.*, *80-690*, 179 pp.

Kirchner, J. W., W. E. Dietrich, F. Iseya, and H. Ikeda (1990), The variability of critical shear stress, friction angle, and grain protrusion in water-worked sediments, *Sedimentology*, *37*, 647–672.

Komar, P. D. (1987), Selective grain entrainment by a current from a bed of mixed sizes: A reanalysis, *J. Sediment. Petrol.*, *57*, 203–211.

Krumbein, W. C. (1938), Size-frequency distributions of sediments and the normal phi curve, *J. Sediment. Petrol.*, *8*, 84–90.

Lustig, L. K. (1965), Sediment yield of the Castaic watershed, Western Los Angeles County California—A quantitative approach, *U.S. Geol. Surv. Prof. Pap.*, *422-F*, 23 pp.

McLean, D. G. (1995), Sensitivity analysis of bedload equations, paper presented at Annual Conference, Can. Soc. of Civ. Eng., Saskatoon, Saskatchewan.

McLean, D. G., M. Church, and B. Tassone (1999), Sediment transport along lower Fraser River: 1. Measurements and hydraulic computations, *Water Resour. Res.*, *35*(8), 2533–2548.

Meyer-Peter, E., and R. Muller (1948), Formulas for bed-load transport, paper presented at Third Conference, Int. Assoc. Hydraul. Res., Stockholm, Sweden.

Milliman, J. D., and R. H. Meade (1983), World-wide delivery of river sediment to the oceans, *J. Geol.*, *91*, 1–21.

Milliman, J. D., and J. P. M. Syvitski (1992), Geomorphic/tectonic control of sediment discharge to the ocean: The importance of small mountainous rivers, *J. Geology*, *100*, 525–544.

Neill, C. R. (1968), A re-examination of the beginning of movement for coarse granular bed materials, report, Hydraul. Res. Stn., Wallingford, U. K.

Paola, C., and R. Seal (1995), Grain size patchiness as a cause of selective deposition and downstream fining, *Water Resour. Res.*, *31*, 1395–1407.

Parker, G., and C. M. Toro-Escobar (2002), Equal mobility of gravel in streams: The remains of the day, *Water Resour. Res.*, *38*(11), 1264, doi:10.1029/2001WR000669.

Parker, G., P. C. Klingeman, and D. G. McLean (1982), Bedload and size distribution in paved gravel-bed streams, *Proc. J. Hydraulics Div. Am. Soc. Civ. Eng.*, *108*, 544–571.

Pitlick, J. (1988), The response of coarse-bed rivers to large floods in California and Colorado, Ph.D. thesis, Colo. State Univ., Fort Collins.

Reid, I., and J. B. Laronne (1995), Bed load sediment transport in an ephemeral stream and comparison with seasonal and perennial counterparts, *Water Resour. Res.*, *31*(3), 773–781.

Shields, A. (1936), Anwendung der aenlichkeitsmechanik und der turbulenzforschung auf die geschiebebewegung, Mitt. der Preussischen Versuchsanstalt fur Wasserbau und Schiffbau, Berlin, Germany.

Singer, M. B., and T. Dunne (2001), Identifying eroding and depositional reaches of valley by analysis of suspended-sediment transport in the Sacramento River, California, *Water Resour. Res.*, *37*(12), 3371–3381.

Stewart, J. H., and V. C. LaMarche (1967), Erosion and deposition produced by the flood of December 1964 on Coffee Creek Trinity County, California, *U.S. Geol. Surv. Prof. Pap.*, *422-K*, 22 pp.

Wathen, S. J., R. I. Ferguson, T. B. Hoey, and A. Werrity (1995), Unequal mobility of gravel and sand in weakly bimodal river sediments, *Water Resour. Res.*, *31*(8), 2087–2096.

White, W. R., W. R. Milli, and A. D. Crabbe (1975), Sediment transport theories: A review, *Proc. Inst. Civ. Eng.*, *59*(2), 265–292.

Wiberg, P. L., and J. D. Smith (1987), Calculations of the critical shear stress for motion of uniform and heterogeneous sediments, *Water Resour. Res.*, *23*(8), 1471–1480.

Wilcock, P. R. (1992), Flow competence: A criticism of a classic concept, *Earth Surf. Processes Landforms*, *17*, 289–298.

Wilcock, P. R. (1996), Estimating local bed shear stress from velocity observations, *Water Resour. Res.*, *32*(11), 3361–3366.

Wilcock, P. R. (2001), Toward a practical method for estimating sediment-transport rates in gravel-bed rivers, *Earth Surf. Processes Landforms*, *26*, 1395–1408.

T. Dunne and M. B. Singer, Donald Bren School of Environmental Science and Management, University of California, Santa Barbara, CA, USA. (bliss@bren.ucsb.edu)